NANO · MICRO small
www.small-journal.com

Carburization of Fe/Ni Catalyst for Efficient Growth of Single-Walled Carbon Nanotubes

*Dewu Lin, Shuchen Zhang, Weiming Liu, Yue Yu, and Jin Zhang**

Scale-up production of single-walled carbon nanotubes (SWNTs) with high quality and purity is in pursuit, since the subsequent post purification treatment of residual metal or amorphous carbon is complicated and restricts further applications. Here, a compatible method to efficiently synthesize pure SWNTs on various supporters by using the precarburized Fe/Ni catalysts is reported. The preparation of catalysts is achieved by gas phase deposition together with CO gas at proper temperature, and the carburization of metal particles occurring simultaneously contributes to the size limitation of catalysts. By using micro-quartz sand as a recyclable supporter, high-quality SWNTs with a yield of 50 mg h^{-1} are prepared with 60% metal precursor utilization, 81% carbon source utilization, and only 0.12% (m/m) metal residues. Taking advantage of carburized Fe/Ni catalysts and appropriate supports makes it possible to balance the quantity, purity, and quality among SWNTs growth. Furthermore, this method provides a straightforward pathway to strongly combine SWNTs and diverse composite materials for further potential applications.

1. Introduction

Single-walled carbon nanotubes (SWNTs) have been regarded as a promising material owing to the unique atomic and electronic structures, and ensuring compelling performance, like mechanical strength,[1] electrical property,[2,3] or thermal conducting.[4] Since the SWNTs were synthesized in 1993, tremendous efforts have been made in the manufacturing of SWNTs with mass production and low cost. However, the prices of bulk pure SWNTs now are still much higher than multi-walled carbon nanotubes (MWNTs) due to the sensitive process control and difficult purification.[5,6]

Currently, catalytic chemical vapor deposition (CVD) has become the most popular method for the synthesis of SWNTs. By elaborated design of the catalyst particles, structure control of SWNTs, such as diameter control,[7,8] electrical type control,[9,10] or even chirality control[11–14] has been developed greatly, and pure SWNTs in good quality were accessible. However, such catalyst engineering was always accompanied by extremely low yield. While the typical high-pressure carbon monoxide (HiPco) method,[15] which could fabricate SWNTs in gas phase with high yield,[6] still remains a challenge in the control of purity, like the obvious metal residue, notable content of MWNT as well as the amorphous carbon. In general, the common problem of SWNTs scale-up synthesis is the decreasing purity along with increasing yield, the following two reasons could be accountable: 1) metal particles tend to assemble together to become larger clusters,[16] and final sizes of clusters are unpredictable especially in gas phase. The clusters with improper size would not contribute to the growth of SWNTs, but catalyze the formation of MWNTs or amorphous carbon, instead. 2) Deactivation of metal catalysts.[5] In the CVD ambient of SWNTs scale-up production, plenty carbon sources were introduced together with the metal precursors at high temperature, so the as-formed metal clusters were surrounded by decomposed carbon species very soon, and would lose the catalytic activity once they were coated with solid carbon shell.

Herein, we first put forward a precarburization treatment of the Fe/Ni catalyst particles to efficiently synthesis pure SWNTs on various substrates or supports. Fe and Ni metals, known as liquid catalyst, have been widely used for SWNTs synthesis because of the high catalytic activity and carbon solubility. However, the migration and aggregation of metal clusters could result in catalysts with broad size distribution. To prevent this effect, precarburization of metal catalysts was applied to suppress the migration by enhancing the combination of metal carbide and base supporters. Moreover, the vapor–liquid–solid mechanism indicates that the carbon species would dissolve in metal catalyst first, then the out coming carbon atoms began to nucleate carbon nanotubes.[17] Thus, an abrupt supply of carbon source at high temperature might cause the deactivation of catalysts by carbon coating, especially during the scale-up production of SWNTs. Therefore, the precarburization of metal catalysts would decrease the risk of catalysts deactivation by shorten the delay between carbon species dissolution and precipitation. Hence, by the combination of precarburized metal catalysts and proper supporters, it is accessible to balance the quantity, purity, and quality among SWNTs scale-up synthesis.

D. W. Lin, Dr. S. C. Zhang, W. M. Liu, Y. Yu, Prof. J. Zhang
Center for Nanochemistry
Beijing Science and Engineering Center for Nanocarbons
College of Chemistry and Molecular Engineering
Peking University
Beijing 100871, China
E-mail: jinzhang@pku.edu.cn

The ORCID identification number(s) for the author(s) of this article can be found under https://doi.org/10.1002/smll.201902240.

DOI: 10.1002/smll.201902240

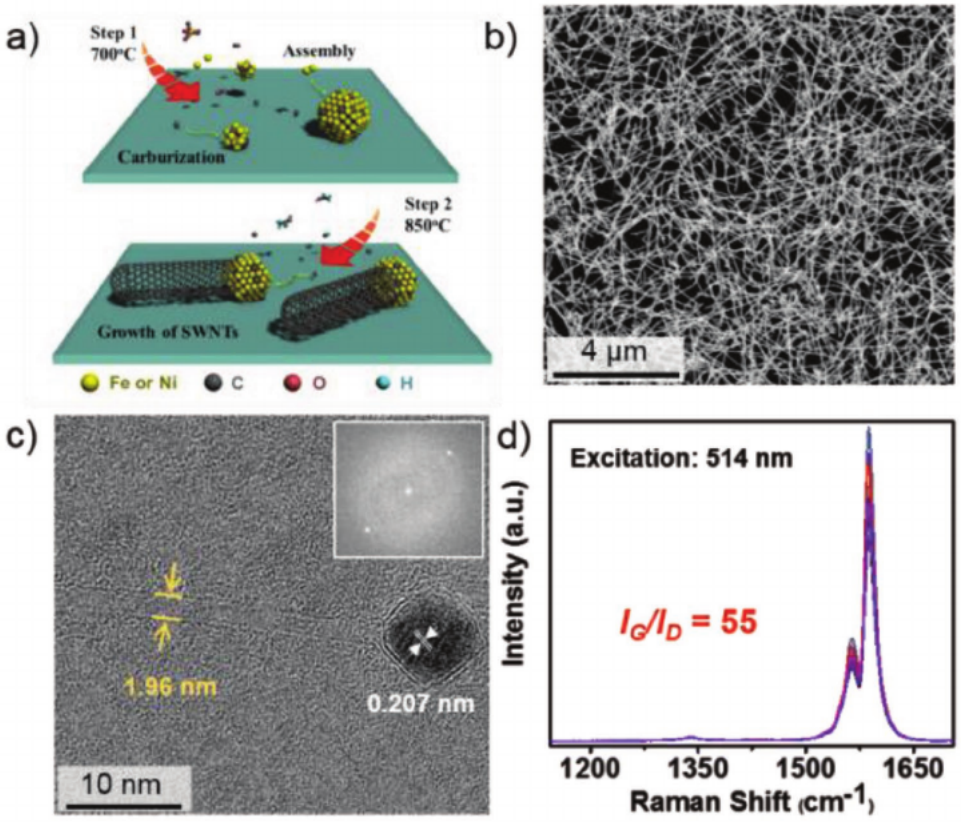

Figure 1. Direct growth of pure SWNTs from the precarburized metal catalysts. a) Schematic showing the procedure designed for deposition of precarburized Fe/Ni catalysts and direct growth of SWNTs. b) SEM image of typical SWNTs based on SiO_2/Si substrate. c) TEM image of a typical SWNT grown from the precarburized Fe/Ni catalyst and corresponding fast Fourier transform of the nanoparticle. d) Raman spectrum of SWNTs from (b), excited by a 514 nm laser.

2. Results and Discussion

The typical process of precarburization of Fe/Ni bimetal catalyst for efficient growth of SWNTs is shown in **Figure 1**a. It has already been detected that commercial carbon monoxide gas was stored in high pressure carbon steel cylinder contained trace amount of transition metal carbonyl,[18] and thus makes it a handy and "natural" metal catalysts precursor diluted by carbon source gas. The commercial CO gas used in our laboratory was detected by inductively coupled plasma mass spectrometry (ICP-MS) method, and only iron and nickel were detected in ppb level (Table S1, Supporting Information). In brief, when the CO and trace amount of metal carbonyl precursors were introduced to the furnace simultaneously at 700 °C, these metal atoms would assemble together to form particles, and the disproportionation of CO would contribute to the precarburization of metal particles. Subsequently, as the temperature rises to 850 °C for SWNTs growth, a dense and clean carbon nanotube film could be obtained on the SiO_2/Si substrate as shown in Figure 1b. The transmission electron microscopy (TEM) image in Figure 1c showed a typical SWNT grown from the catalyst particle. And the catalyst particle was connected to SWNT in perpendicular mode,[19] which was in accordance with the behavior of liquid metal with notable carbon solubility. The well-crystallized particle showed the interplanar spacing of 0.207 nm, which is consistent with carbide phase.[20] The impurity and defects in SWNTs would affect the corresponding Raman signal obviously, therefore the Raman intensity ratio between G band and D band was usually used to estimate the quality of SWNTs samples.[21] An I_G/I_D value of 55 shown in Figure 1d indicates a well-crystallized graphitic structure of as-grown SWNTs.

To characterize the precarburized Fe/Ni catalysts in detail, a 10 nm thick SiN film grid was chosen as the substrate for catalysts deposition. The TEM image in **Figure 2**a shows clearly that the final catalyst particles deposited on substrates were presented in limited size, and the average diameter was 2.17 nm according to the size distribution (Figure 2c). High-resolution transmission electron microscopy (HRTEM) of typical catalyst particles revealed the interplanar spacing of 0.207 and 0.209 nm, which was consistent with the as-grown catalysts in Figure 1c. However, the structural similarity of metallic Fe/Ni and the carbide would result in the challenge of identification. Significantly, the carburization of metal catalyst particles had been observed directly by using the SiN film grid as support. The energy-dispersive X-ray spectroscopy (EDS) mapping (Figure 2d) analyses of a catalyst particle after carburization at 700 °C revealed that the Fe and Ni mapping images have the same shape as the particle. And even the C mapping image had an imprecise shape due to the disturbance of random carbon deposition on grid, the carburization of Fe and Ni at 700 °C was unambiguous according to previous reports.[22]

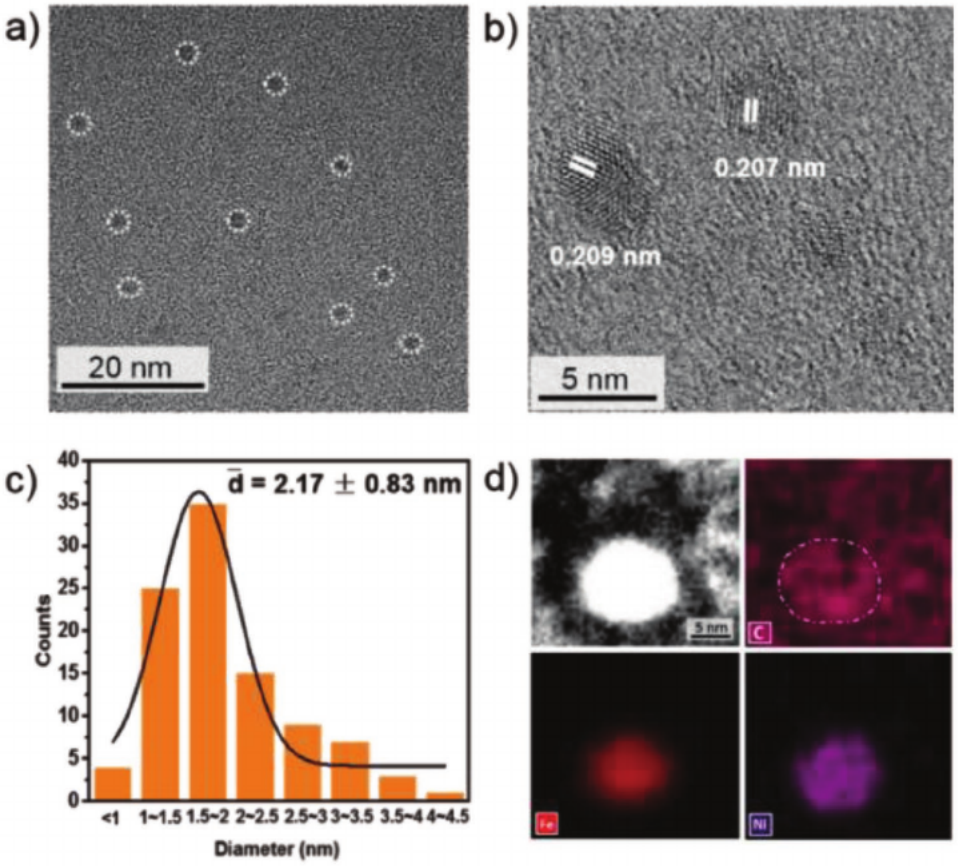

Figure 2. Characterization of the precarburized Fe/Ni catalysts. a) TEM image of precarburized Fe/Ni catalysts. b) HRTEM of the precarburized Fe/Ni catalysts. c) Corresponding size distribution of catalysts in (a) with mean diameter of 2.17 nm. d) High-angle annular dark-field imaging-scanning transmission electron microscopy-EDS mapping images of the precarburized Fe/Ni catalyst, indicating the component of Fe, Ni, and C.

It is well accepted that substrates or supports with numerous steps or kinks tended to anchor the catalyst particles on the substrate surface, and this is clearly shown in Figure S1 in the Supporting Information. The corresponding statistics of particle sizes indicated that the catalyst particles in steps (3.71 nm) were also much smaller than that on the flatten surface (8.56 nm), because the metal catalyst particles were easier to migrate on the flatten surface, and subsequently would combine with others or probably be anchored when trapped by steps or kinks on the surface. Significantly, the carburized catalyst particles were found unlikely to migrate even in the reducing atmosphere (**Figure 3**). The carburized Fe/Ni catalysts were deposited on the ST-cut quartz substrates using commercial CO gas as precursor. The incipient catalyst particles at 700 °C had the average diameter of 2.25 nm. After reduction at 850 °C for 5 min, the average diameter increased by 41% to 3.18 nm (Figure 3e). And when the reduction time was prolonged to 10 min, the average diameter of as-obtained catalysts increased by another 5.7% to 3.36 nm (Figure 3f). To get a better sense of such result, reduction of Fe metal catalysts was prepared as comparison (Figure S2, Supporting Information). The diameter of Fe metal catalysts after reduction increased by 140% to 6.62 nm when compared with the original iron oxide (2.76 nm). While the diameter of precarburized metal catalysts increased by only 63% to 4.50 nm. Hence, it was demonstrated that the carburization could restrain the migration and aggregation of metal catalysts, and the lower surface energy of carbide compared to metal might account for it.

As the aggregation of catalyst on substrates could be restrained by precarburization, the deposition of metal catalysts from CO gas played the important role in the control of catalysts development. Atomic force microscope (AFM) characterizations in Figure S3 in the Supporting Information unambiguously indicated that the density of catalyst particles increased with the time of exposure to CO gas at 700 °C, and simultaneously, the size of catalyst particles developed from 1.67 nm of 1 min exposure to 2.76 nm of 5 min and 4.97 nm of 10 min gradually. The average size of particles increases near linearly over time (Figure S4, Supporting Information), providing the feasibility for the accurate control of catalyst particles. In addition, the similar particles development was observed on the SiO_2/Si substrates (Figure S5, Supporting Information), demonstrating the potential controllability of catalyst particles on various substrates or supports.

Furthermore, the iron and nickel carbonyl precursors would be sufficiently cracked above 325 °C, and the generated metal atoms would form catalyst particles then. While the disproportion of CO catalyzed by iron group metal had been observed at around 700 °C.[23] Thus, the temperature at which the thermal cracking of CO and carburization of Fe/Ni catalyst occurred was optimized. Scanning electron microscope (SEM) images

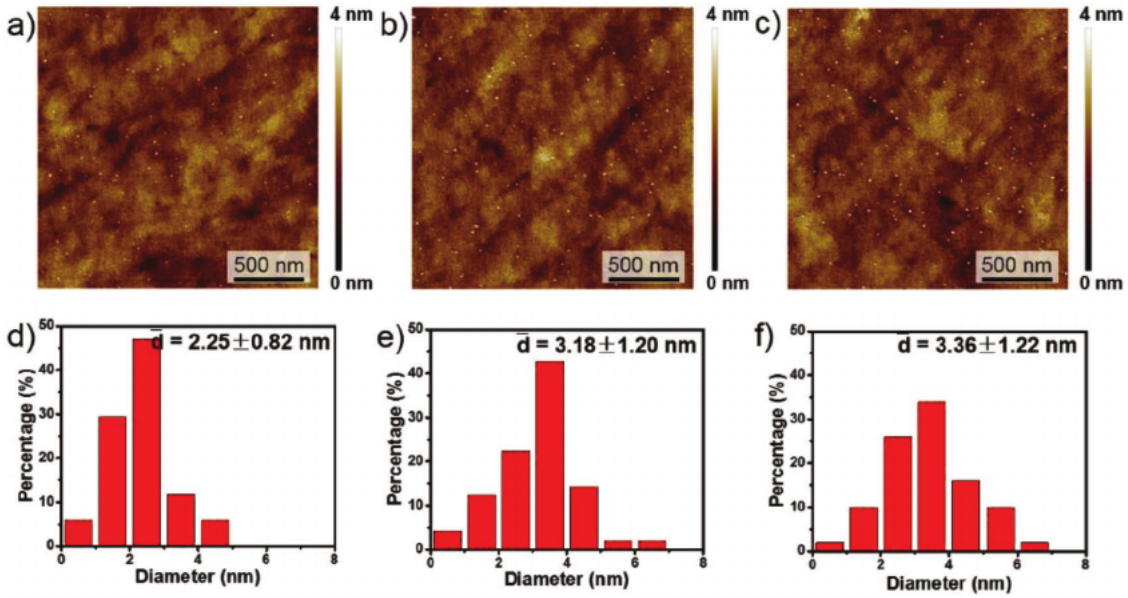

Figure 3. AFM characterization of carburized Fe/Ni catalyst particles deposited on quartz substrate. a) Deposition at 700 °C; b) deposition at 700 °C and reduction at 850 °C for 5 min; c) deposition at 700 °C and reduction at 850 °C for 10 min. d–f) Corresponding catalyst particles size distribution.

in Figure S6a–c in the Supporting Information indicated that SWNTs with long length and high density were obtained on SiO_2/Si substrates as CO mixed with trace amount of iron and nickel carbonyl precursors were introduced at 700 °C. Moreover, the optimized temperature for the following SWNTs growth was 850 °C according to the results in Figure S6d–f.

In order to grow SWNTs in scale-up yield, pure quartz sands of micro size were chosen as the support and used in a vertical furnace as shown in Figure S7 in the Supporting Information, the details of SWNTs growth were described in the Supporting Information. In brief, the annealed quartz sand of micro size was put in the vertical tube which was embedded with a quartz filter in the middle, so that sufficient gas flow would blow up the quartz sand. As the CO gas flowed through the floating quartz sand at 700 °C, Fe/Ni catalyst particles would form on the surface of quartz sand uniformly. Subsequent growth of SWNTs was achieved using ethanol as carbon source at 850 °C. The original obtained sample is shown in **Figure 4**a, white

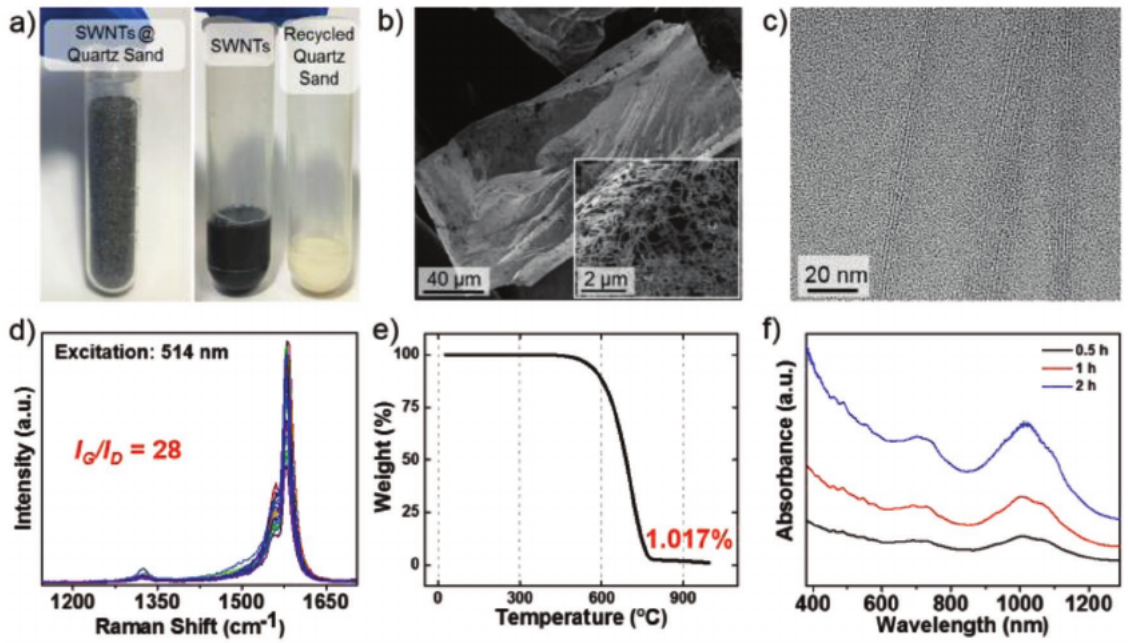

Figure 4. Scale-up production of SWNTs using quartz sand as supporter. a) Optical image of SWNTs based on quartz sand, collected SWNTs, and recycled quartz sand. b) SEM image of SWNTs based on quartz sand. c) TEM image of the collected SWNTs deposited on carbon film. d) Raman spectrum excited by a 514 nm laser. e) TGA data (ramp rate, 10 °C min^{-1}) of a 3.5 mg collected SWNTs in air. f) Absorption spectrum of the collected SWNTs.

quartz sand became totally black after growth. Later, SWNTs were collected by ultrasonic washing the obtained sample in 0.3% (m/m) hydrogen fluoride aqueous solution, leaving behind recyclable quartz sands. The SEM images in Figure 4b showed that the quartz sand was fully covered by SWNTs, of which the length were about 4 μm. TEM image of SWNTs bundle in Figure 4c demonstrated the single-wall structure of nanotubes with less defects and impurities. Other TEM images of the individual SWNT in Figure S9 in the Supporting Information distinctly showed the intact structure of as-obtained SWNT. A typical Raman spectrum in Figure 4d showed an average I_G/I_D value of 28, indicating the high quality of such collected SWNTs. In addition, the thermal gravimetric analysis (TGA) (Figure 4e) of such SWNTs before any purification showed only 1.017% residues remained after heating above 800 °C, indicating a high purity when considering about the possible exfoliation of SiO_2 supports during washing. And the peak height decreasing occurred at 560 °C, which was in accordance with reported SWNTs combustion temperature, suggesting the high quality of SWNTs synthesized on quartz sand using precarburized Fe/Ni particles as catalyst. While as a reference, the commercial arc-SWNTs were characterized by Raman and TGA as well. The average I_G/I_D value of commercial arc-SWNTs was about 13 (Figure S8a, Supporting Information), and the TGA showed in Figure S8b in the Supporting Information indicated the notable impurity in it. And the quantity of obtained SWNTs was found to increase with the prolongation of growth time, as shown in Figure 4f, the absorbance increased obviously, indicating the development of SWNTs quantity. On average, the yield of SWNTs synthesized on quartz sand using carburized Fe/Ni particles as catalyst was 50 mg h^{-1}.

Pure SWNTs with few metal catalyst residues are the promising goal of SWNTs scale-up production. X-ray photoelectron spectroscopy characterization of the collected SWNTs indicated that no apparent metal was detected (Figure S10, Supporting Information). Quantitative metal element analysis with ICP-MS detected 0.12% metal impurity, meaning carbon purity was more than 99.8% (Table S2, Supporting Information). As the iron and nickel carbonyl precursors were introduced with 100 sccm CO for 60 min, based on the concentration of metal carbonyl detected in Table S1 in the Supporting Information, the total quantity of introduced metal was 309.9 μg, indicating the metal carbonyl precursors' utilization of ≈60%. The concentration of ethanol carbon source in argon carrier gas was detected by gas chromatography in Figure S11 in the Supporting Information, which means the 1.97×10^{-7} mol ethanol in 150 μL input gas. Thus, the utilization of carbon atoms was 81% during the 60 min synthesis of SWNTs on quartz sand using carburized Fe/Ni particles as catalyst.

Different substrates or supports were also examined immediately. **Figure 5** shows the typical SEM images of SWNTs, when the CO gas with metal carbonyl precursors was introduced at about 700 °C, Fe/Ni catalyst particles would anchor on surface of these substrates or supports, then it was handy to synthesize SWNTs at an appropriate temperature subsequently. Raman spectrum of the respective SWNTs was shown in Figure S12 in the Supporting Information. The SWNTs horizontal array of relatively high density was obtained on the ST-cut quartz substrate (Figure 5a). And the surfaces of NaCl particles were covered by crowded SWNTs, which provided a convenient, clean, and nondestructive pathway for the scale-up production of SWNTs due to

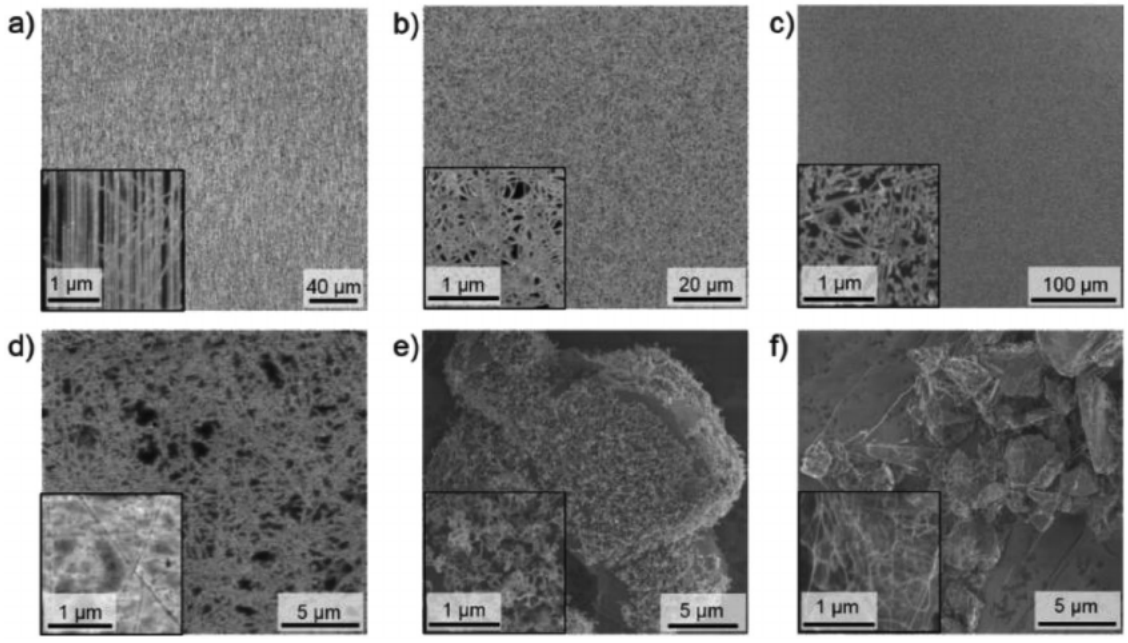

Figure 5. SEM images of abundant SWNTs directly synthesized on various substrates or supports. a) SWNTs on ST-cut quartz substrate. b) SWNTs on SiO_2/Si substrate. c) SWNTs on mica substrate. d) SWNTs on sapphire substrate. e) SWNTs on the surface of NaCl particles. f) SWNTs across the silicon particles.

the solubility of NaCl in water (Figure 5e). Carbon nanotubes network could be directly synthesized among silicon particles to make SWNTs/Si composites for further application in energy field (Figure 5f).

3. Conclusion

In conclusion, we have developed a precarburization method for Fe/Ni catalyst to efficiently synthesize SWNTs with few metal residues for the first time. Precarburization of Fe/Ni bimetal catalyst at lower temperature would contribute to restrain the aggregation of metal catalysts, and decrease the risk of carbon-coating catalysts deactivation potentially by shorten the delay between carbon dissolution and precipitation. The application of appropriate substrates helps to control the diffusion and following assembly of metal catalyst. By using quartz sand as support in the newly designed vertical furnace, 50 mg h^{-1} high-quality SWNTs were fabricated with 60% metal precursors utilization, 81% carbon source utilization, and only 0.12% (m/m) metal residues. Nevertheless, directly combining the SWNTs with multifunctional composite materials may pave the way for future large-scale application of SWNTs.

4. Experimental Section

Synthesis of SWNTs by Precarburized Fe/Ni Catalysts on SiO_2/Si Substrate: The pure SWNTs films were synthesized by a two-step ethanol CVD method. First is the deposition of Fe/Ni catalysts: a SiO_2/Si substrate with 300 nm oxide layer was placed in 1 in. quartz tube followed by a 5 min purge of 300 sccm argon. After the furnace was heated to 700 °C under an Ar/H_2 (300 sccm/200 sccm) gas flow, a 10 sccm CO gas contained ppb level of Fe/Ni carbonyl was introduced instead of hydrogen for 2 min. During this process, precarburized Fe/Ni nanoclusters of appropriate size were assembled on SiO_2/Si substrate. Then the furnace was heated to 850 °C under an Ar/H_2 (300 sccm/200 sccm) flow, and 100 sccm argon through an ethanol bubbler was introduced as the carbon source in the next 15 min. Afterward, the furnace was cooled down to room temperature in argon and hydrogen atmosphere.

Supporting Information

Supporting Information is available from the Wiley Online Library or from the author.

Acknowledgements

This work was supported by the Ministry of Science and Technology of China (2016YFA0200101 and 2016YFA0200104), the National Natural Science Foundation of China (grant nos. 21233001, 21790052 and 51720105003).

Conflict of Interest

The authors declare no conflict of interest.

Keywords

carbon nanotubes, carburization, efficiency, metal catalysts, migration

Received: May 3, 2019
Revised: June 16, 2019
Published online: July 2, 2019

[1] Y. Bai, R. Zhang, X. Ye, Z. Zhu, H. Xie, B. Shen, D. Cai, B. Liu, C. Zhang, Z. Jia, S. Zhang, X. Li, F. Wei, *Nat. Nanotechnol.* **2018**, *13*, 589.
[2] G. J. Brady, A. J. Way, N. S. Safron, H. T. Evensen, P. Gopalan, M. S. Arnold, *Sci. Adv.* **2016**, *2*, e1601240.
[3] C. Qiu, Z. Zhang, M. Xiao, Y. Yang, D. Zhong, L.-M. Peng, *Science* **2017**, *355*, 271.
[4] D. Suh, C. M. Moon, D. Kim, S. Baik, *Adv. Mater.* **2016**, *28*, 7220.
[5] M. Kumar, Y. Ando, *J. Nanosci. Nanotechnol.* **2010**, *10*, 3739.
[6] S. Jiang, P. X. Hou, M. L. Chen, B. W. Wang, D. M. Sun, D. M. Tang, Q. Jin, Q. X. Guo, D. D. Zhang, J. H. Du, K. P. Tai, J. Tan, E. I. Kauppinen, C. Liu, H. M. Cheng, *Sci. Adv.* **2018**, *4*, eaap9264.
[7] G. Chen, Y. Seki, H. Kimura, S. Sakurai, M. Yumura, K. Hata, D. N. Futaba, *Sci. Rep.* **2015**, *4*, 3804.
[8] S. Zhang, L. Tong, Y. Hu, L. Kang, J. Zhang, *J. Am. Chem. Soc.* **2015**, *137*, 8904.
[9] S. Zhang, Y. Hu, J. Wu, D. Liu, L. Kang, Q. Zhao, J. Zhang, *J. Am. Chem. Soc.* **2015**, *137*, 1012.
[10] J. Wang, X. Jin, Z. Liu, G. Yu, Q. Ji, H. Wei, J. Zhang, K. Zhang, D. Li, Z. Yuan, J. Li, P. Liu, Y. Wu, Y. Wei, J. Wang, Q. Li, L. Zhang, J. Kong, S. Fan, K. Jiang, *Nat. Catal.* **2018**, *1*, 326.
[11] S. Zhang, L. Kang, X. Wang, L. Tong, L. Yang, Z. Wang, K. Qi, S. Deng, Q. Li, X. Bai, F. Ding, J. Zhang, *Nature* **2017**, *543*, 234.
[12] J. R. Sanchez-Valencia, T. Dienel, O. Gröning, I. Shorubalko, A. Mueller, M. Jansen, K. Amsharov, P. Ruffieux, R. Fasel, *Nature* **2014**, *512*, 61.
[13] F. Yang, X. Wang, D. Zhang, J. Yang, D. Luo, Z. Xu, J. Wei, J.-Q. Wang, Z. Xu, F. Peng, X. Li, R. Li, Y. Li, M. Li, X. Bai, F. Ding, Y. Li, *Nature* **2014**, *510*, 522.
[14] S. Zhang, X. Wang, F. Yao, M. He, D. Lin, H. Ma, Y. Sun, Q. Zhao, K. Liu, F. Ding, J. Zhang, *Chem* **2019**, *5*, 1182.
[15] P. Nikolaev, M. J. Bronikowski, R. K. Bradley, F. Rohmund, D. T. Colbert, K. A. Smith, R. E. Smalley, *Chem. Phys. Lett.* **1999**, *313*, 91.
[16] C. Lu, J. Liu, *J. Phys. Chem. B* **2006**, *110*, 20254.
[17] A. J. Page, Y. Ohta, S. Irle, K. Morokuma, *Acc. Chem. Res.* **2010**, *43*, 1375.
[18] T. C. Williams, C. R. Shaddix, *Combust. Sci. Technol.* **2007**, *179*, 1225.
[19] M. He, Y. Magnin, H. Amara, H. Jiang, H. Cui, F. Fossard, A. Castan, E. Kauppinen, A. Loiseau, C. Bichara, *Carbon* **2017**, *113*, 231.
[20] R. Anton, *Carbon* **2009**, *47*, 856.
[21] L. Qingwen, Y. Hao, C. Yan, Z. Jin, L. Zhongfan, *J. Mater. Chem.* **2002**, *12*, 1179.
[22] C. T. Wirth, B. C. Bayer, A. D. Gamalski, S. Esconjauregui, R. S. Weatherup, C. Ducati, C. Baehtz, J. Robertson, S. Hofmann, *Chem. Mater.* **2012**, *24*, 4633.
[23] P. E. Nolan, D. C. Lynch, A. H. Cutler, *Carbon* **1994**, *32*, 477.